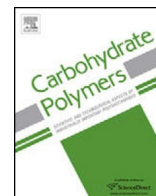




Contents lists available at ScienceDirect

## Carbohydrate Polymers

journal homepage: [www.elsevier.com/locate/carbpol](http://www.elsevier.com/locate/carbpol)

## In vitro evaluation of glycol chitosan based formulations as oral delivery systems for efflux pump inhibition



Delia Mandracchia<sup>a</sup>, Adriana Trapani<sup>a,\*</sup>, Giuseppe Tripodo<sup>b</sup>, Maria Grazia Perrone<sup>a,\*</sup>, Gaetano Giammona<sup>c</sup>, Giuseppe Trapani<sup>a</sup>, Nicola Antonio Colabufo<sup>a</sup>

<sup>a</sup> Department of Pharmacy-Drug Sciences, University of Bari "Aldo Moro", Via Orabona 4, 70125 Bari, Italy

<sup>b</sup> Department of Drug Sciences, University of Pavia, Viale Taramelli 12, 27100 Pavia, Italy

<sup>c</sup> Department of "Scienze e Tecnologie Biologiche, Chimiche, Farmaceutiche (STEBICEF)", University of Palermo, via Archirafi 32, Palermo 90123, Italy

### article info

#### Chemical compounds studied in this article:

2- iminothiolane (PubChem CID: 433941)

Rhodamine 123 (PubChem CID 65217)

L-Cysteine hydrochloride (PubChem CID: 60960)

dl-Dithiothreitol (PubChem CID: 446094)

5,5'-Dithiobis(2-nitrobenzoic acid)

(PubChem CID: 6254)

Sodium tripolyphosphate (PubChem CID: 244455)

#### Keywords:

Glycol chitosan-based formulations

P-gp inhibition properties

Rhodamine 123

Glycol chitosan-4-thiobutylamidine

thiomer

Caco-2 cells

Oral bioavailability

### abstract

Recently, we have reported that glycol chitosan (GCS) was able to reverse the P- glycoprotein (P-gp) efflux pump. The objective of the present study was to evaluate the potential of two GCS-based dosage forms (aqueous solution or nanoparticle suspension) for oral administration of the P-gp substrate Rho-123. A further aim of the present study was to assess the effect of the glycol chitosan-4-thiobutylamidine thiomers (GCS-TBA) on P-gp activity considering that the corresponding thiomers of chitosan series is a well-known P-gp inhibitor. Pre-treatment of Caco-2 cell monolayer with a GCS solution or GCS-based nanoparticles increased the absorptive transport of Rho-123 across the monolayer of 1.43-fold. The modification of GCS with 2-iminothiolane led to GCS-TBA conjugate which did not show any P-gp inhibitory activity. Therefore, GCS polymer and corresponding dosage forms may contribute to increase the oral bioavailability of Pgp-substrate drugs, while GCS-TBA cannot be used for the same purpose.

© 2017 Published by Elsevier Ltd.

### 1. Introduction

The 170 kDa P-glycoprotein (P-gp), also known as multidrug resistance (MDR) protein 1 (MDR-1), is a transmembrane protein located in several biological tissues including the apical membrane of hepatocytes, the apical lumen of the gastrointestinal enterocytes and the luminal membrane of brain capillary endothelial cells (Benet, Izumi, Zhang, Silverman, & Wachter, 1999; Chan, Lowes, & Hirst, 2004; Juliano & Ling, 1976). It is most involved in MDR mechanisms, working as efflux pump for most drugs decreasing

so their cellular uptake. In fact, several drugs are substrates of P-gp and actively transported back to the apical side determining so a higher concentration outside of the cell and, consequently, limiting the bioavailability and the therapeutic potential of these substances (Cordon-Cardo et al., 1990; Thiebaut et al., 1987). Classic P-gp substrates are structurally different drugs including anti-cancer agents, antibiotics, and antivirals. Therefore, inhibition of P-gp efflux pump really influences the absorption of important classes of drugs and it is because this topic attracted the attention of most researchers. From a drug delivery view point, there are two main applications for which it is essential to inhibit efflux pumps, specifically those involving oral and brain delivery. In fact, taking into account that *i*) the P-gp is most expressed in the intestinal tract (Hunter & Hirst, 1997) and *ii*) the oral route is one of the most

\* Corresponding authors.

E-mail addresses: [adriana.trapani@uniba.it](mailto:adriana.trapani@uniba.it) (A. Trapani), [mariagrazia.perrone@uniba.it](mailto:mariagrazia.perrone@uniba.it) (M.G. Perrone).

convenient administration pathway of drugs enabling high patient compliance, inhibition of efflux pump mediated transport in the intestinal tract may allow the delivery of a wide variety of drugs P-gp substrates by this administration route. Thus, for instance, to improve the absorption through the intestine of most P-gp substrate anticancer drugs, these agents must be orally administered in combination with inhibitors of the efflux pump (Mazzafarro, Bouchemal, & Ponchel, 2013a,2013b). Similarly, inhibition of P-gp drug efflux system increases the permeability of a broad spectrum of drugs through the blood-brain barrier (BBB) where P-gp is also most expressed. Actually, BBB protects the brain from harmful substances but, at same time, limits the brain delivery of most P-gp substrate neuroactive drugs. Thus, co-administration of anticancer drugs and P-gp inhibitors allows brain accumulation and the treatment of brain tumors which still represents one of the biggest challenges in anticancer therapy (Tang et al., 2012).

Regarding P-gp inhibitors, over the past decades a wide range of chemically different substances have been identified including both small molecules and polymeric substances (Colabufo et al., 2008; Werle, 2008). However, most of the low molecular weight P-gp inhibitors gave rise to pharmacokinetic interactions with the substrates of the efflux pump and, using this first generation of such inhibitors, disappointing results were obtained in clinical trials. Next generations of P-gp inhibitors (e.g. valspodar, elacridar, zosuquidar) were developed with better clinical outcome. Nevertheless, most of these low molecular weight P-gp inhibitors suffer from undesired pharmacodynamic side effects due to high concentrations necessary for adequate inhibition of P-gp. They, indeed, often bring about chronic toxicity and side effects such as bradycardia and immunosuppression (Britton & Palacios, 1982; Pennock et al., 1991). In contrast, among the polymeric inhibitors, a number of pharmaceutical excipients such as Cre-mophor EL, Polyethylene glycols (PEGs), Tweens, Myrj, Vitamin E derivatives (D- $\alpha$ -tocopheryl polyethylene glycol succinate, also known as TPGS) and copolymers of ethylene oxide and propylene oxide (Pluronic) are included and they, in general, are devoid of any biological activity. In fact, polymeric P-gp inhibitors possess the advantage of remaining at the adsorption site and, being not adsorbed, provide no or negligible systemic toxic side effects and, therefore, are safe enough.

In recent years, attention has been paid to thiolated polymers (referred to also as "thiomers") namely hydrophilic polymers containing free thiol groups on their backbone for their improved mucoadhesive, cohesive, enzyme inhibitory and permeation enhancing properties very useful in pharmaceutical field for transmucosal delivery (Bernkop-Schnurch, 2004). Moreover, it has also been shown, both *in vitro* and *in vivo*, that thiomers are endowed with interesting P-gp inhibitory properties (Bonengel & Bernkop-Schnürch, 2014). Thus, for instance, in the most studied series of chitosan (CS)-based thiomers, it has been demonstrated that, in the presence of CS-4-thiobutylamidine (CS-TBA) with or without GSH, the absorption of the Pgp-substrate Rhodamine 123 (Rho-123) across freshly excised rat intestine was 3-fold higher than that observed in buffer alone, while Myrj 52 was able to provide a lower improvement (i.e., 1.8-fold) (Foger, Schmitz, & Bernkop-Schnurch, 2006).

We have recently reported that the glycol chitosan (GCS)-based thiomers GCS-*N*-acetyl-cysteine (GCS-NAC) 400 kDa was also able to reverse *in vitro* the P-gp efflux pump and rehabilitate the fluorescent probe Rho-123 cell entrance (Trapani et al., 2014). In addition, unlike the unmodified CS, also GCS 400 kDa as such was able to rehabilitate Rho-123 cell entrance and reverse P-gp (Trapani et al., 2014). Therefore, GCS, a CS derivative endowed with good mucoadhesive performances and water-soluble at neutral/acidic pH values, represents a new example of nontoxic polymer characterized by P-gp inhibitory properties (Trapani et al., 2014).

The aim of the present study was to evaluate the potential of GCS-based dosage forms such as GCS containing aqueous solution or a suspension of nanoparticles (NPs) constituted by GCS for oral administration of the model P-gp substrate Rho-123. In fact, since it is reported that NPs may bypass the drug-resistance mechanism (Dong et al., 2009; Wong et al., 2006), we hypothesized that such nanostructured formulation may improve the P-gp inhibition properties of GCS. For this purpose, the effects on the Rho-123 transport after a pre-treatment of Caco-2 cells with a GCS solution or with a GCS-based NP suspension were studied. Moreover, in an attempt to maximize the P-gp inhibitory properties of GCS, we designed and synthesized the conjugate obtained by reaction of GCS with 2-iminothiolane, that is GCS-4-thiobutylamidine (GCS-TBA), to evaluate its efflux pump inhibition properties, taking into account that, as mentioned above, the corresponding thiomers of CS series (i.e., CS-TBA) is reported to be a very efficient P-gp inhibitor (Foger et al., 2006). The GCS-TBA conjugate was synthesized and characterized from a spectroscopic (FT-IR,  $^1\text{H}$  NMR) point of view and thiol group content (Ellman's assay) as well as for its interaction with P-gp using Caco-2 cells. Furthermore, the swelling and mucoadhesive properties of the GCS-TBA conjugate were assessed considering that the presence of the cationic amidine moiety should increase the electrostatic interactions with the negative functional groups of the mucins (Trapani et al., 2014). The obtained results are herein reported and discussed also in the light of the accepted inhibitory mechanisms of P-gp efflux.

## 2. Materials and methods

### 2.1. Materials

All chemicals were of analytical grade unless otherwise stated. Glycol chitosan (GCS, Mw 400 kDa, degree of deacetylation = 83% according to manufacturer instructions), 2-iminothiolane (IT, Traut's reagent), L-cysteine hydrochloride anhydrous >99.5% (Cys), DL-dithiothreitol 99.5% (DTT), 5,5'-dithiobis(2-nitrobenzoic acid) (DTNB, Ellman's reagent), pentasodium tripolyphosphate (TPP), porcine stomach mucin (type II, bound sialic acid ~ 1%), rhodamine-123, phosphate-buffered saline (PBS), D<sub>2</sub>O, dimethyl sulfoxide (DMSO) and 3-(4,5-dimethylthiazol-2-yl)-2,5-diphenyltetrazolium bromide (MTT) were purchased from Sigma-Aldrich (Milan, Italy). Dialysis tubes with a MWCO 12–14 kDa (Spectra/Por) were purchased from Spectrum Labs. Throughout this work, double-distilled water was used. Cell culture reagents were purchased from Celbio s.r.l. (Milano, Italy). Culture Plate 96/wells plates were purchased from Perkin Elmer Life Science; Millicell-96 wells for P-gp transport assay were purchased from Merck Millipore. Caco-2 cells were a gift of Dr. Aldo Cavallini and Dr. Caterina Messa from the Laboratory of Biochemistry, National Institute for Digestive Diseases, "S. de Bellis", Bari (Italy). Caco-2 cells were grown in Dulbecco's Modified Eagle's Medium (DMEM) high glucose supplemented with 10% fetal bovine serum, 2 mM glutamine, 100 U/mL penicillin, 100  $\mu\text{g}/\text{mL}$  streptomycin, in a humidified incubator at 37 °C with a 5% CO<sub>2</sub> atmosphere.

### 2.2. Apparatus

FT-IR spectra (KBr pellets) were recorded in the range 4000–400  $\text{cm}^{-1}$  using a Perkin Elmer 1600 IR Fourier Transform Spectrophotometer (Monza, Italy). The resolution was 1  $\text{cm}^{-1}$ . UV-vis analyses were performed using a Perkin Elmer Spectrometer Lambda 25, Perkin Elmer, (Monza, Italy) in KBr disks.  $^1\text{H}$  NMR spectra were recorded in D<sub>2</sub>O using a Varian Mercury 300 MHz instrument.  $^{13}\text{C}$  NMR spectra were recorded in D<sub>2</sub>O using an Agilent 500-nmrs 500 MHz instrument. DSC thermograms were

recorded using a Mettler Toledo DSC 822e Stare 202 System apparatus and 5 mg of each sample in aluminium pans without pin. The samples were heated from 25 °C to 250 °C at a rate of 5 °C min<sup>-1</sup> under a nitrogen flow of 50 cm<sup>3</sup> min<sup>-1</sup>. Indium (purity 100%) was used for calibrating temperature. Lyophilizations were performed using a Christ Alpha 1-4 LSC instrument at 59 °C and 0.016 mBar. The average diameters and zeta potential of GCS-based nanoparticles were measured by a Zetasizer Nano ZS instrument (Malvern Instruments Ltd., Worcestershire, UK) and, in particular for the zeta potential, after sample dilution with KCl 1 mM (Mattoli Belmonte et al., 2014).

### 2.3. Preparation of GCS-based dosage forms

The GCS solution dosage form was prepared dissolving 2.5 mg of polysaccharide in 2.5 mL of bi-distilled water. The suspension of GCS-based NPs was prepared following the ionic gelation method using TPP as crosslinking as previously reported (Di Gioia et al., 2015). Briefly, to a solution of GCS in aqueous AcOH (0.1% v/v, 0.75 mL), an aqueous solution of TPP (0.07%, w/v, 0.8 mL) was added under magnetic stirring to induce the ionic gelation of the polycation. The resulting NPs were isolated by centrifugation (16,000 g, 45 min), re-suspended in ultrapure water and characterized for size, zeta potential and polydispersity index by photon correlation spectroscopy (PCS) using a Zetasizer Nano ZS (Zen 3600, Malvern, UK).

### 2.4. Synthesis of N-(4-1-iminobutylthio)-glycol chitosan (GCS-TBA) conjugate

To a solution of 250 mg of GCS in distilled water (50 mL), IT (67.2 mg, 0.488 mmol) was added under stirring at room temperature (r.t.) and under a nitrogen atmosphere. The pH of reaction mixture was adjusted at pH 7 with NaOH 1 N and the stirring was prolonged at room temperature for 20 h. Then, the pH was regulated at 8.0 and DTT (231 mg, 1.5 mmol) was added and the solution stirred for further 3 h. After this time, the pH was fixed at 4.5 by HCl 1N and the solution was dialyzed for 3 days against acidic distilled water (pH 4.5) containing 1% (w/v) of NaCl for first 24 h and for further 2 days without NaCl. The resulting solution was lyophilized and the resulting GCS-TBA conjugate was obtained as a white solid in 86% (w/w) yield that was stored at 4 °C until further use. FT-IR (KBr:  $\nu_{\max}$  cm<sup>-1</sup>): 3400 (O-H str, OH); 2922 (C-H str.), 1635 (C=O str, C-NH<sub>2</sub><sup>+</sup>). <sup>1</sup>H NMR (400 MHz, D<sub>2</sub>O,  $\delta$ ): 1.8–2.1 (m, CH<sub>3</sub>, acetyl); 2.5–2.7 (m, C<sup>2</sup>H-NH<sub>2</sub>); 2.8–3.1 (m, C<sup>2</sup>H-NH-C(CH<sub>2</sub>-) = NH<sub>2</sub><sup>+</sup>). <sup>13</sup>C NMR (500 MHz, D<sub>2</sub>O), ppm: 177.58 (C=O carboxymethyl), 156.43 (R-NH-C-NH<sub>2</sub><sup>+</sup> Cl<sup>-</sup>, 4-mercaptobutanimidamide bonded to GCS), 98.75 (C1 GCS), 76.82 (C4 GCS), 74.69 (C5 GCS), 71.62 (C3 GCS), 69.48 (R-O-CH<sub>2</sub>-CH<sub>2</sub>-OH GCS), 60.28 (R-O-CH<sub>2</sub>-CH<sub>2</sub>-OH GCS), 55.94 (C2 GCS), 26.57 (R-CH<sub>2</sub>-CH<sub>2</sub>-CH<sub>2</sub>-SH 4-mercaptobutanimidamide bonded to GCS), 22.05 (R-C(=O)-CH<sub>3</sub> GCS).

The shape of GCS-TBA conjugate was assessed by Transmission electron microscopy (TEM). Briefly, TEM investigation was performed with a Jeol-Jem-1200EXII. Samples were prepared by casting a drop of a GCS-TBA dispersion (1 mg/mL) in Milli-Q water at pH 4.0 onto carbon-coated copper grids and left drying at 25 °C in a dessicator and then negatively stained with uranyl acetate and analyzed. For TEM studies, GCS-TBA conjugate was dispersed in acidified water (pH 4.0) to prevent thiol oxidation before deposition on the carbon-coated copper grids.

### 2.5. Determination of the thiol group content in N-(4-1-iminobutylthio)-glycol chitosan (GCS-TBA) conjugate by Ellman's assay

The amount of thiol groups on GCS-TBA conjugate (i.e., the thiol modification degree) was determined with Ellman's reagent following a reported method (Bernkop-Schnürch, Hornof, & Zoidl, 2003) with slight modifications. Briefly, the Ellman's reagent was prepared by dissolving DTNB (6 mg) in 0.5 M phosphate buffer pH 8.0 (20 mL). Then, 1 mL of Ellman's reagent was added to 1 mL of GCS-TBA water solution (5 mg in 2.5 mL of distilled water) and the obtained solution diluted with bi-distilled water to a GCS-TBA final concentration of 0.5 mg/mL. The mixture was stirred for 2 h at r. t. and the absorbance of supernatant was measured at 424 nm wavelength. The amount of thiol groups on GCS-TBA conjugate was calculated from a standard curve obtained by glycol chitosan solution with increasing amount of l-cysteine HCl.

### 2.6. Swelling properties of N-(4-1-iminobutylthio)-glycol chitosan (GCS-TBA) conjugate

The swelling properties of GCS-TBA conjugate were determined by a gravimetric method reported in literature with minor modifications (Muzzalupo et al., 2001). Exactly weighed aliquots of GCS-TBA were placed on a 5 mL centrifuge glass tube pierced in the lower part to allow medium elimination upon centrifugation and provided with a sintered glass filter ( $\varnothing$  10 mm; porosity: G3). The tube containing the sample was left to swell at 37 °C by immersing it in a beaker containing the liquid medium, i.e. double-distilled water, HCl 0.1 N (pH 1.2) and phosphate buffer solution (PBS) pH 7.4. At scheduled time intervals the excess of liquid was removed by percolation at atmospheric pressure, then the filter was placed in a properly sized centrifuge test tube, centrifuged at 3000 rpm for 5 min and weighed. The filter tare was determined after centrifugation with pure water alone. The weight swelling ratio (q) was calculated as:

$$q = W_s/W_d$$

where  $W_s$  and  $W_d$  are the weights of the swollen and dry sample, respectively. All the experiment was carried out at room temperature in triplicate and the results were in agreement within  $\pm$  3%.

### 2.7. In vitro evaluation of N-(4-1-iminobutylthio)-Glycol Chitosan (GCS-TBA) conjugate mucoadhesive properties

The mucoadhesive properties of GCS-TBA conjugate were determined in comparison with those of parent polymer (GCS) and Carbopol 934 following a turbidimetric method already employed by us (Mandrachia et al., 2011; Pitarresi, Pierro, Tripodo, Mandrachia, & Giammona, 2005; Trapani et al., 2014) using poly(acrylic acid), as a positive control (Thermes et al., 1992). Briefly, mucin (10 mg) was dispersed in PBS (pH 6.8, 10 mL) and the mixture was kept at 37 °C for 24 h under stirring (150 rpm). Then, appropriate amounts of GCS, or GCS-TBA or poly(acrylic acid) (Carbopol 934) were added to the mucin dispersion (mucin/polymer weight ratio equal to 1) and each sample was incubated at 37 °C under stirring (150 rpm) for 2, 5, 8, 15 or 24 h. After each incubation time, the transmittance (%) of the samples was recorded at 650 nm using a Perkin-Elmer (Milan, Italy) Lambda Bio20 spectrophotometer. Each experiment was performed in triplicate and the results are reported as mean  $\pm$  SD.

## 2.8. Caco-2 cell viability assay carried out in the presence of GCS-TBA conjugate

Determination of cell growth was performed using the MTT assay at 3 h. This method is based on the ability of viable cells to metabolize MTT, a water-soluble salt (yellow color), by cellular oxidoreductase into a water-insoluble blue formazan product. Therefore, the amount of formazan produced is proportional to the viable cells. Briefly, viable cells (30000/well) were plated into sterile 96-Well Cell Culture Cluster (Corning, NY 14831) and incubated with 5 mg/mL of GCS-TBA at 37 °C in 5% CO<sub>2</sub>. After 3 h of incubation, the culture medium was replaced by a solution of MTT 0.5 mg/mL (Sigma-Aldrich, Milan, Italy) in PBS (Sigma-Aldrich, Milan, Italy). After 2 h incubation at 37 °C in 5% CO<sub>2</sub> this solution was removed and 200 µL of DMSO was added to each well to dissolve the formazan product. Absorbance values at 570 nm were measured using a plate reader Victor V3 (Perkin-Elmer) and DMSO medium was used as blank solution. The experiment was carried out in triplicate.

## 2.9. Permeability experiments

Preparation of Caco-2 monolayer. Caco-2 cells were seeded onto a Millicell® assay system (Millipore), where a cell monolayer is set in between a filter cell and a receiver plate, at a density of 30,000 cells/well. The culture medium was replaced every 48 h and the cells kept for 21 days in culture. The Trans Epithelial Electrical Resistance (TEER) of the monolayers was measured daily, before and after the experiment, using an epithelial voltohometer (Millicell-ERS). Generally, TEER values greater than 1000 U for a 21 day culture are considered optimal.

## 2.10. Drug transport experiments

After 21 days of Caco-2 cell growth, the medium was removed from filter wells and from the receiver plate, which were filled with fresh Hanks' balanced salt solution [HBSS, pH 7.4 (HBSS buffer, Invitrogen)]. This procedure was repeated twice, and the plates were incubated at 37 °C for 30 min.

Apical to basolateral ( $P_{app}$ , AB) and basolateral to apical ( $P_{app}$ , BA) permeability of drugs were measured at 120 min (Colabufo et al., 2008; Colabufo, Berardi, Cantore et al., 2010; Colabufo, Berardi, Perrone et al., 2010; Leopoldo et al., 2006). Drugs were dissolved in HBSS, pH 7.4 and sterile filtered.

For tested compounds and Rho-123  $P_{app}$  evaluation, Caco-2 cells monolayer was incubated with *GCS solution* or *GCS-based nanoparticles* (2.5 mg/mL in DMEM medium) or *GCS-TBA* (5 mg/mL in DMEM medium) or Rho-123 ( $1 \times 10^{-4}$  M) at 37 °C for 120 min.

While, for Rho-123  $P_{app}$  evaluation after 24 h incubation of Caco-2 cells monolayer with *GCS solution* or *GCS-based nanoparticles* (2.5 mg/mL in DMEM medium) or *GCS-TBA* (5 mg/mL in DMEM medium), the medium was removed from filter wells and from the receiver plate and Rhodamine solution ( $1 \times 10^{-4}$  M) was added to the filter wells (75 µL) and the receiver wells (250 µL per well) and the plates were incubated at 37 °C for 120 min.

After 120 min incubation samples were removed from the apical (filter well) and basolateral (receiver plate) side of the monolayer and were stored in a freezer (-20 °C) pending analysis. The concentration of tested compounds was measured using UV spectroscopy. The apparent permeability ( $P_{app}$ ), in units of nm per second, was calculated using the following equation:

$$P_{app} = \frac{V_A}{\text{Area} \times \text{time}} \times \frac{[\text{drug}]_{\text{acceptor}}}{[\text{drug}]_{\text{initial}}}$$

where  $V_A$  is the volume (in mL) in the acceptor well; Area is the surface area of the membrane (0.11 cm<sup>2</sup> of the well); time is the

total transport time in seconds (7200 s);  $[\text{drug}]_{\text{acceptor}}$  is the concentration of the drug measured by UV spectroscopy;  $[\text{drug}]_{\text{initial}}$  is the initial drug concentration in the apical or basolateral wells.

## 2.11. Analytical methods

Samples from *in vitro* permeation studies were analyzed by using a Shimadzu- spectrophotometer, UV-1800. The wavelength for UV adsorbance was set as follows: 224 nm for *GCS solution* or *GCS-based nanoparticles*, 230 nm for *GCS-TBA* and 500 nm for Rho-123.

## 2.12. Statistical analysis

Results are expressed as mean  $\pm$  S.D. Significance was calculated using a one-way ANOVA and differences were considered significant at 95% level of confidence ( $p < 0.05$ ) using GraphPad Prism v. 4.00 computer program (GraphPad Software, Inc. CA, USA). Bonferroni tests were used for post-hoc contrast.

# 3. Results

## 3.1. Synthesis and analytical characterization of GCS-TBA conjugate

With the aim to increase the P-gp inhibition properties of GCS, we prepared the conjugate GCS-TBA, an analogous thiomere of CS-TBA which is known to possess optimal inhibition properties of the efflux pump in the CS series (Foger et al., 2006). The modification of GCS was achieved by reaction of the polysaccharide with the Traut's reagent, IT, following the synthetic route employed for CS-TBA with slight modifications (Bernkop-Schnürch et al., 2003). In particular, the GCS polymer was allowed to react with IT in distilled water (Fig. 1) and, to minimize the oxidation reaction of thiol groups, the reducing agent DTT was added to the mixture according to a previously published procedure (Pitarresi et al., 2005). The reaction was carried out at r.t. for 20 h and then the mixture was dialyzed and lyophilized.

GCS-TBA conjugate was characterized by FT-IR and <sup>1</sup>H NMR spectroscopy. In particular, FT-IR (KBr) spectrum of GCS-TBA showed an intense absorption band at 1635 cm<sup>-1</sup> due to the stretching of amide carbonyl (Fig. 2). The broad band at 3400 cm<sup>-1</sup> was assigned to the stretching of hydroxyl group, overlapping the N-H stretching in the same region. The thermogram of the GCS-TBA conjugate resulted very different from that of the parent polymer (Trapani et al., 2014), showing a rather broad peak at about 135 °C and a more sharp endothermic peak at 220 °C (Fig. 2). The <sup>1</sup>H NMR spectrum clearly showed two multiplets centered at  $\delta$  1.89 and at  $\delta$  2.87 assigned to the acetyl and C<sup>2</sup>H-NH-C(CH<sub>2</sub>) = NH<sub>2</sub><sup>+</sup> protons, respectively. <sup>13</sup>C NMR showed two detectable new peaks (with respect to unfunctionalized GCS) at 156.43 ppm and 26.57 ppm attributable to the 4-mercaptobutanimidamide chain from the 2-iminothiolane moiety bonded to GCS. In particular, the peak at 156.43 ppm was attributed to the R-NH-C=NH<sub>2</sub><sup>+</sup>Cl<sup>-</sup> as the imidamide carbon could be usually found at around 150–160 ppm. The peak at 26.57 ppm belongs to the R-CH<sub>2</sub>-CH<sub>2</sub>-CH<sub>2</sub>-SH carbon (Fig. 2).

The <sup>1</sup>H NMR (D<sub>2</sub>O) spectrum of GCS-TBA conjugate compared to that of the parent polymer (Fig. 3) showed a clear shift of the proton signal at 2-position of amino-glucose ring resonating at  $\delta$

2.5–2.7 in the parent polymer to  $\delta$  2.8–3.1 in GCS-TBA, confirming so the conjugate formation between GCS and IT.

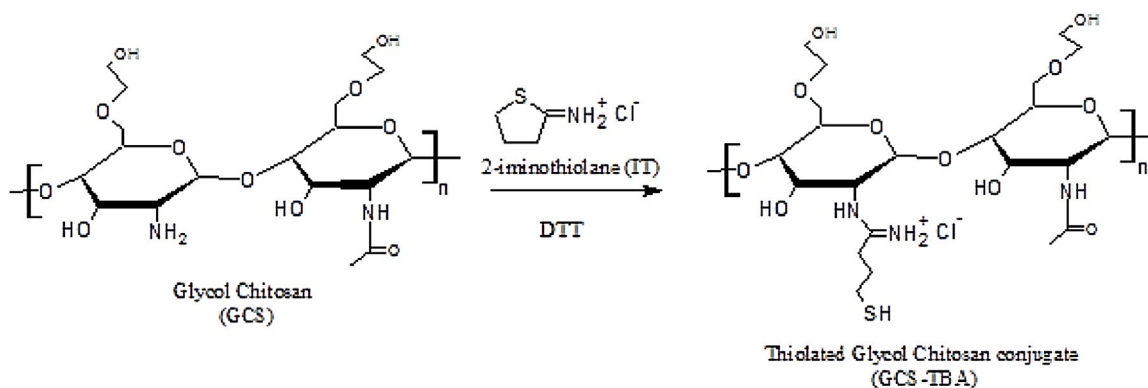


Fig. 1. Synthetic route for the preparation of the GCS-TBA thiomers.

Derivatization degree (DD% mol) was calculated by comparing the integral of the proton at 2-position of amino-glucose using the following Eq. (1):

$$DD\% = \frac{\int_{\text{C}^2\text{H} - \text{NH} - \text{C} = \text{NH}_2 +}{\int_{\text{C}^2\text{H} - \text{NH} - \text{C} = \text{NH}_2 + 1/3 \int_{\text{CH}_3\text{CO}}} \times 100 \quad (1)$$

and resulted of  $89 \pm 1\%$  mol/mol.

The content of thiol groups in GCS-TBA conjugate was determined by Ellman's assay (Bernkop-Schnürch et al., 2003) and it resulted of  $110 \mu\text{mol/g}$ .

### 3.2. In vitro evaluation of swelling and mucoadhesive properties of N-(4-1- iminobutylthio) glycol chitosan (GCS-TBA) conjugate

Taking into account that swelling properties strongly influence the mucoadhesive performance of polymers (Trapani et al., 2014), a study of GCS-TBA swelling features was carried out at two different concentrations (i.e., 10 mg/mL and 20 mg/mL) and pH values by a gravimetric method and the results are also shown in Fig. 4A and B. Statistically significant differences in swelling ratios were observed elapsing the time at higher concentration (20 mg/mL) in water as well as in PBS pH 7.4 as solvents with variations of these ratios up to 60%–80% between 1 h and 21 h. On the other hand, the corresponding differences in swelling ratios at 10 mg/mL resulted not significant from a statistical point of view in the same solvents with variations of the ratios of about 15% at most. Moreover, at 20 mg/mL the ratios clearly decreased elapsing the time in acidic medium at pH 1.2 in statistically significant way with a reduction of the swelling ratio of about 95% between 1 h and 21 h. Instead, at 10 mg/mL we did not observe such decrease in swelling ratio in acidic medium but a slight increase even though of about 20% only between 1 h and 21 h. It seems from these results that at lower concentration the changes in swelling ratios are, on the whole, marginal/borderline while, at the higher one, they are indicative enough of extensive swelling. Consistent with this suggestion, it was observed that at the higher concentration (20 mg/mL) of GCS-TBA and in PBS pH 7.4 there was a faster tendency to hydrogel formation as proved using the tube inverting method (Li, Cho, Kwon, Janát-Amsbury, & Huh, 2013). As confirmed by TEM analysis and photon correlation spectroscopy (PCS) (Fig. 5A and B, respectively), GCS-TBA dispersions form aggregated superstructures sized less than  $1 \mu\text{m}$ .

The mucoadhesive properties of GCS-TBA conjugate were evaluated and the results are shown in Fig. 4C. In particular, the interaction studies between GCS-TBA conjugate and mucin were performed in PBS (pH 6.8) following a turbidimetric method already employed by us (Mandracchia et al., 2011; Pitarresi et al., 2005; Trapani et al., 2014). Due to the formation of macro-aggregates,

as a consequence of polymer–mucin interaction, the transmittance value decreases by increasing this interaction (Rossi, Ferrari, Bonferoni, & Caramella, 2000).

As shown in Fig. 4C, GCS-TBA conjugate exhibited transmittance values slightly lower than those observed for GCS polymer. Hence,

the thiolated glycol chitosan conjugate GCS-TBA should interact with mucin stronger than the native GCS, probably due to the presence of the SH groups able to interact with mucin glycoproteins via thiol-disulfide exchange reactions. However, at the same time, it was observed that the transmittance values of GCS and GCS-TBA were higher than those of polyacrylic acid used as control. Taking also into account the results of the previous work (Trapani et al., 2014), these results suggested that, GCS and GCS-TBA should possess good mucoadhesive characteristics but, in any case, lower than those of Carbopol 934 (Thermes et al., 1992).

### 3.3. Transport studies on GCS-based dosage forms

The required two GCS-based formulations designed for the study i.e., an aqueous GCS solution (2.5 mg/mL) and a GCS-based NPs suspension were at first prepared. In particular, the former dosage form was obtained by simple dissolution of the polymer in the required amount of the solvent, the latter was prepared by ionic gelation method using TPP as crosslinking agent (Di Gioia et al., 2015). The mean diameters of the prepared NPs were of  $291 (44) \text{ nm}$  and the polydispersity index of  $0.36 (0.02)$  suggesting a broad particle distribution (Di Gioia et al., 2015). As expected, the surface charge of these NPs was positively charged [i.e.,  $18.6 (2.2)$ ] (Di Gioia et al., 2015).

Both the GCS solution (2.5 mg/mL) and the GCS-based NPs suspension (2.5 mg/mL) were tested on the high level efflux pump P-gp expressing Caco-2 cell monolayer to determine their *Papp* (B-A/A-B) value and the corresponding results are listed in Table 1. As shown, low efflux ratios (i.e., *Papp* B-A/*Papp* A-B ratio) were observed for both the solution and the NPs suspension (i.e., 2.87 and 1.1, respectively) as well as for the known P-gp substrate Rho-123 (i.e., *Papp* value of 2.3). Moreover, the effects on the bidirectional transport of Rho-123 across Caco-2 cell monolayer after 18 h incubation of Caco-2 cells with GCS solution (2.5 mg/mL) or with GCS-based nanoparticle suspension (2.5 mg/mL) were measured and the corresponding results are also shown in Table 1.

The pre-treatment with the solution or the suspension decreased the *Papp* of Rho-123 both in the A-B (from  $484 \text{ nm/sec}$  to  $263 \text{ nm/sec}$ ) and B-A direction (from  $1130 \text{ nm/sec}$  to  $874 \text{ nm/sec}$ ) and it corresponds to 1.43-fold increase compared to the control (Table 1).

Therefore, based on these transport experiments, it can be concluded that the P-gp inhibitory activity of GCS-based nanoparticles should be greater than that of GCS solution, as deduced by their

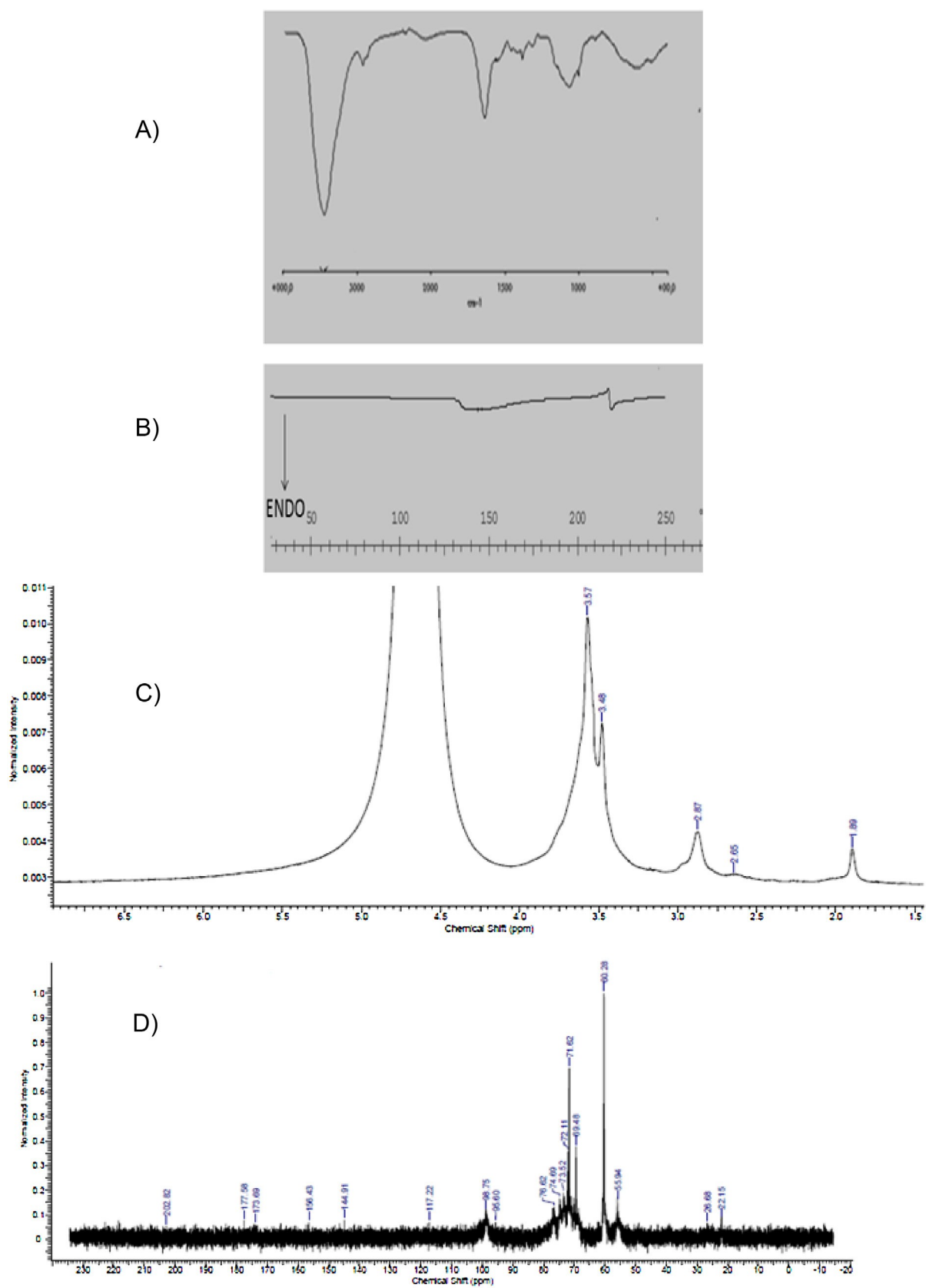


Fig. 2. A) FT-IR spectrum and B) DSC thermogram of GCS-TBA conjugate; C) <sup>1</sup>H NMR spectrum and D) <sup>13</sup>C NMR spectrum of GCS-TBA conjugate.

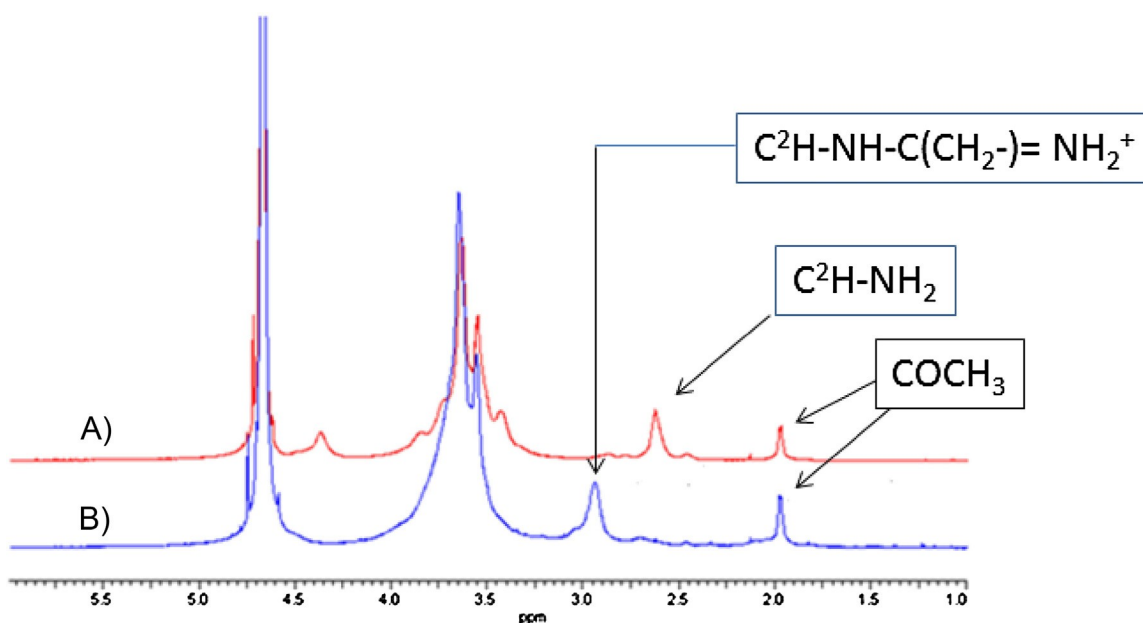


Fig. 3.  $^1\text{H}$  NMR spectrum of A) GCS and B) GCS-TBA conjugate.

**Table 1**

Apparent permeability of tested compounds across Caco-2 cell monolayers overexpressing human P-gp from the basolateral to apical (BA) sides and from the apical to basolateral (AB) compartments.

Papp BA/AB	Papp BA (nm/sec)	Papp AB (nm/sec)	h (nm)	s ( $\text{M}^{-1} \text{cm}^2$ )
GCS-based nanoparticles (2.5 mg/mL)				
1.1	0.19	0.15	224	0.687
GCS solution (2.5 mg/mL)				
2.87	0.535	0.174	224	0.687
GCS-TBA solution (5 mg/mL)				
16.8	1125	67	230	95
Rho 123				
2.3	1130	484	500	75,297
Rho (18 h incubation with GCS-based nanoparticles, 2.5 mg/mL)				
3.3	874	263	500	75,297
Rho (18 h incubation with GCS solution, 2.5 mg/mL)				
3.3	874	263	500	75,297
Rho (18 h incubation with GCS-TBA solution, 5 mg/mL)				
2.2	874	394	200	75,297

Papp (B-A/A-B) values (*i.e.*, 1.1 vs 2.87, respectively). However, even if the nanosized formulation should be more advantageous than the solution one to obtain efficient P-gp inhibition, essentially no difference occurs between the two GCS dosage forms when the effects of their pre-treatment on the Rho-123 transport are compared. In fact, both showed the same Papp (B-A/A-B) value (*i.e.*, 3.3) after 18 h incubation (Table 1).

The GCS-TBA conjugate was also tested on Caco-2 cells monolayer to determine its Papp (BA/AB) to evaluate its effect on the transport P-gp mediated. As reported in Table 1, a high efflux ratio was observed for GCS-TBA (*i.e.*, 16.8) and this result suggests that the conjugate should not possess P-gp inhibition properties but it should behave almost as a substrate of the efflux protein. Indeed, it is accepted that BA/AB ratios in the range 18–20 and <2 are indicative of substrates and inhibitors, respectively, while modulators are denoted by BA/AB values ranging from 2 to 18 (Colabufo, Berardi, Cantore et al., 2010). In fact, GCS-TBA Caco-2 cells pre-treatment was totally ineffective towards Rho-123 transport (BA/AB = 2.2), just confirming that GCS-TBA behaves as a P-gp substrate, as demonstrated by its high BA/AB value (16.8) (Table 1).

MTT test was carried out in order to assess that during GCS-TBA transport experiment incubation cell viability was preserved. Only 27% cytotoxicity in 3 h incubation time was observed (data not shown).

#### 4. Discussion

The development of drugs with good oral or brain bioavailability represents an important challenge in pharmaceutical field (Pang et al., 2016; Trapani et al., 2004). For efficient oral and brain delivery, MDR – particularly MDR-1, P-gp is a major obstacle because it may determine a higher concentration outside of the target cell of drugs limiting so their bioavailability and therapeutic potential. Therefore, inhibition of these efflux pumps can lead to enhanced absorption of drugs across the intestine as well as to improve the brain penetration of useful drugs such as anticancer agents. In this context, our previous findings, indicating that GCS polymer is endowed with P-gp inhibitory properties, led us to evaluate the effect of GCS-based dosage forms for oral administration of the model P-gp substrate Rho-123. Since it is reported that NPs

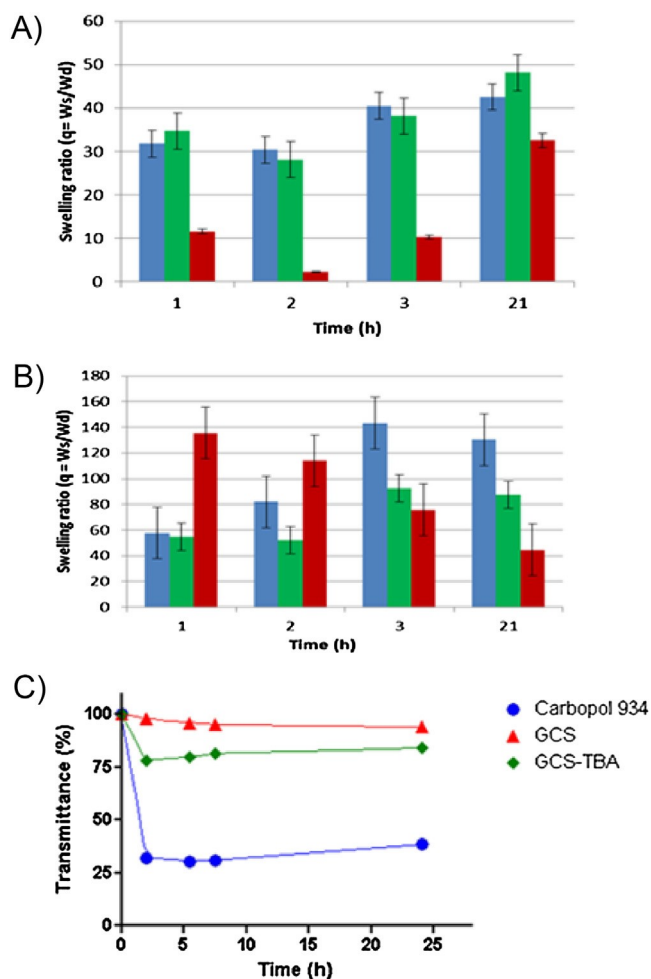


**Fig. 4.** A) swelling at 10 mg/mL in water (blue bars), in PBS pH 7.4 (green bars) and at pH 1.2 (red bars); B) swelling at 20 mg/mL in water (blue bars), in PBS pH 7.4 (green bars) and at pH 1.2 (red bars); C) Transmittance values (%) at 650 nm of mucin dispersions in the presence of GCS (2), GCS-TBA conjugate (C) and Carbopol 934 (●) as a function of the incubation time. (For interpretation of the references to colour in this figure legend, the reader is referred to the web version of this article.)

may bypass the drug-resistance mechanism (Dong et al., 2009; Wong et al., 2006), we selected a GCS-based nanoparticle formulation to evaluate the effect of a pre-treatment of Caco-2 cells with this dosage form on the transport of the model P-gp substrate Rho-123 compared with that of a promptly prepared GCS aqueous solution. The results reported in Table 1 clearly show that, even though the nanostructured formulation should be characterized by better inhibitory P-gp properties compared to GCS solution on the basis of their  $Papp$  (B-A/A-B) values, essentially no difference occurs between the two dosage forms as for the effects of their pre-treatment on the Rho-123 transport. In such case, the pre-treatment with the promptly prepared GCS solution should be of choice compared to the nanostructured formulation taking into account both the very simple preparation procedure of solution and the possible toxicity concerns that nanomaterials may show (Zhao et al., 2013). However, it cannot be ruled out that, with P-gp substrates different from Rho-123, different outcomes could be observed and, according to the  $Papp$  (B-A/A-B) values, the pre-treatment with the nanostructured dosage form could be more advantageous than the solution one in order to obtain efficient P-gp inhibition. As for the GCS-TBA, our findings indicate that this conjugate, as hydrogel, is characterized by a condensed structure that may be due to the chemical cross-linking of the thiolated GCS-TBA in aqueous solution. Thus, for instance, thiol groups located close

on different polymer chains can quickly form disulfide bonds and, therefore, the polymer chains result cross-linked through intermolecular disulfide bonds (Dünnhaupt et al., 2012). However, we believe that the condensed structure of GCS-TBA may be also due to the network resulting from intra- or inter-molecular interactions between the thiol and the amidine groups of the conjugate as shown in Fig. 5C. It should be remembered that, being the  $pK_a$  of alkyl thiols in the range of 8–10, the thiomers GCS-TBA will be more reactive at physiological pH values leading to electrostatic interactions between polymer chains (Dünnhaupt et al., 2012). This suggestion is in agreement with the swelling experiments indicating an increase of the swelling ratios at physiological pH values and at 20 mg/mL concentration of conjugate, while a reduction of the swelling ratios occurs at pH 1.2 at the same concentration. This decrease of the ratios should be due to the protonation of thiol groups occurring in acidic environment which prevents the network formation leading to faster degradation of the polymer and/or disulfide bond rupture determining so the elimination of soluble portions of the polymer. It should be noted that at 21 h the swelling ratio of 20 mg/mL and pH 1.2 is almost the same of the sample at 10 mg/mL. Similarly, the condensed structure of GCS-TBA may also account for its mucoadhesive properties very different from those of Carbopol 934 despite the GCS-TBA conjugate is characterized by the presence of the cationic amidine moiety which should increase the electrostatic interactions with the negative functional groups of the mucins. Indeed, the condensed structure of GCS-TBA and the consequent decreased macromolecular flexibility may prevent an efficient interpenetration with mucus protein chains (Trapani et al., 2014).

On the other hand, conversely to the corresponding conjugate with the poorly water-soluble at physiological pH CS polymer (*i.e.*, CS-TBA), the efflux ratio observed for GCS-TBA (*i.e.*, 16.8) does rule out any P-gp inhibitory properties by the latter conjugate. To rationalize this unexpected result, the proposed P-gp inhibition mechanisms of polymeric substances as GCS-TBA and GCS should be considered and they are summarized in Fig. 6 (Chen et al., 2015; Gupta, Garg, Tanmay, & Arora, 2015; Li et al., 2014; Werle, 2008). Concerning GCS, a water-soluble at neutral/acidic pH values chitosan derivative, we hypothesized an interaction between the terminal OH groups of GCS ethylene glycol moieties and the polar heads of the Caco-2 cell membranes disturbing their fluidity (Trapani et al., 2014). It may be possible that the condensed structure of GCS-TBA and the consequent decreased macromolecular flexibility prevents an efficient interaction between the terminal ethylene glycol moieties and the polar heads of the Caco-2 cell membranes accounting for the P-gp inhibition inactivity of this thiomers. That is, it is possible that the hydrogel formation may block the interaction between GCS-TBA and Caco-2 cells. Thus, in the GCS series, an appropriate macromolecular flexibility should be necessary for establish the interaction with the cell membranes leading to changes of membrane fluidity. In this context, it is interesting to note that, to overcome MDR in cancer, NPs based on the thiolated glycol chitosan obtained from GCS and sulfosuccinimidyl-6-(3'-[2-pyridylidithio]-propionamido) hexanoate (sulfo-LC-SPDP) (Fig. 5D) were loaded with P-gp silencing gene. Likely, this last thiomers, structurally similar to GCS-TBA, is devoted of appropriate macromolecular flexibility and, hence, of significant P-gp inhibitory activity (Lee et al., 2012; Yhee et al., 2015). On the other hand, the condensed structure of GCS-TBA may also prevent the formation of disulfide bonds between the-SH and cysteine-moieties of P-gp, which is the accepted mechanism of P-gp inhibition by thiomers (Fig. 6) (Gupta et al., 2015). However, to account for the GCS-TBA P-gp inhibition inactivity, besides the alteration in membrane fluidity and integrity or the interaction with the cysteine-moieties of P-gp, further mechanisms including the inhibition of P-gp ATPase activ-



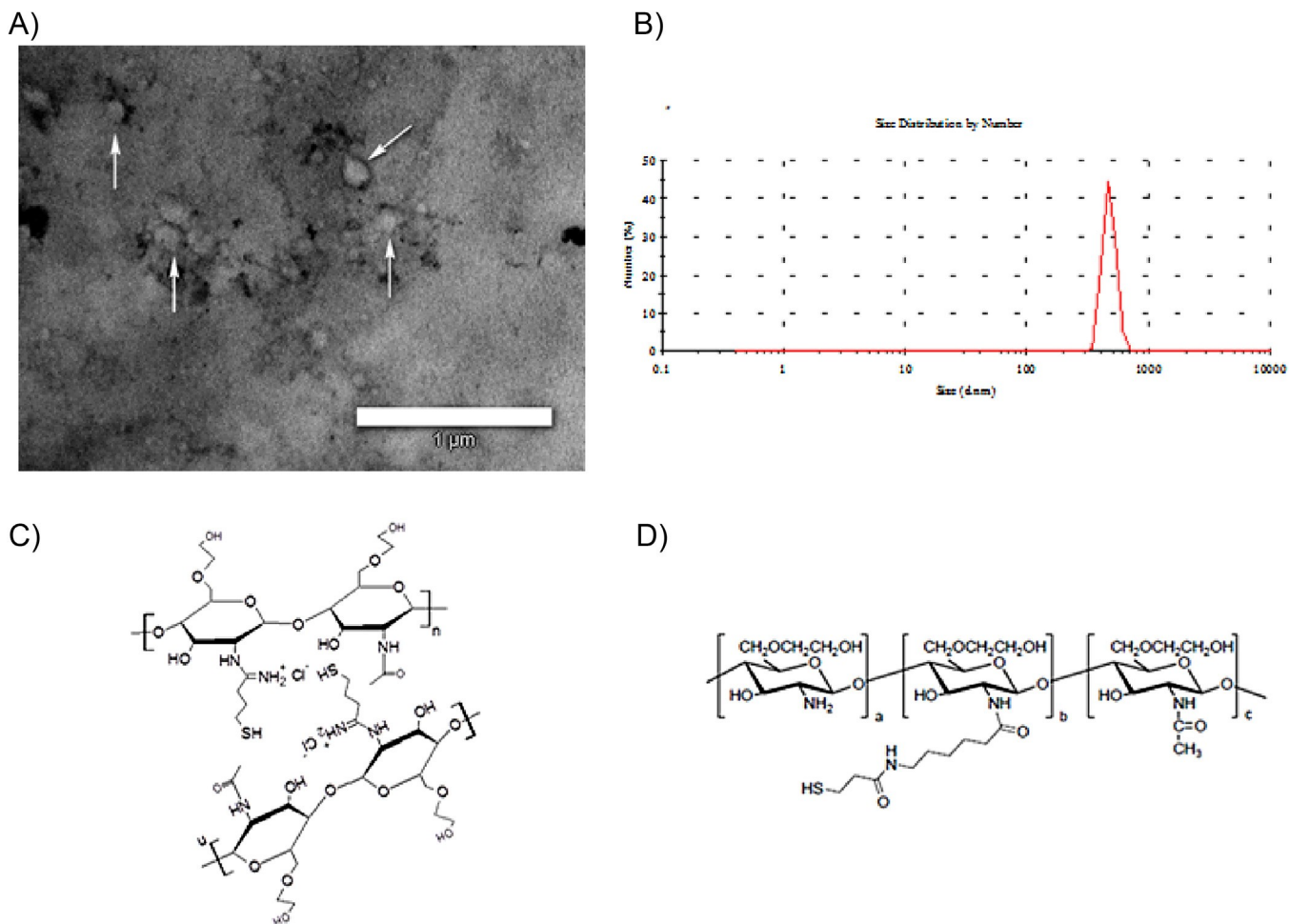


**Fig. 5.** A) TEM images of GCS-TBA (1 mg/mL, pH 4) (bar 1 μm); B) Size distribution graph of GCS-TBA determined by PCS; C) Schematic intra- or inter-molecular interactions between the thiol and the amidine groups of the conjugate GCS-TBA; D) Chemical structure of the thiomers obtained from GCS and sulfosuccinimidyl-6-(3'-[2-pyridyldithio]propionamido) hexanoate (sulfo-LC-SPDP) (Lee et al., 2012; Yhee et al., 2015).

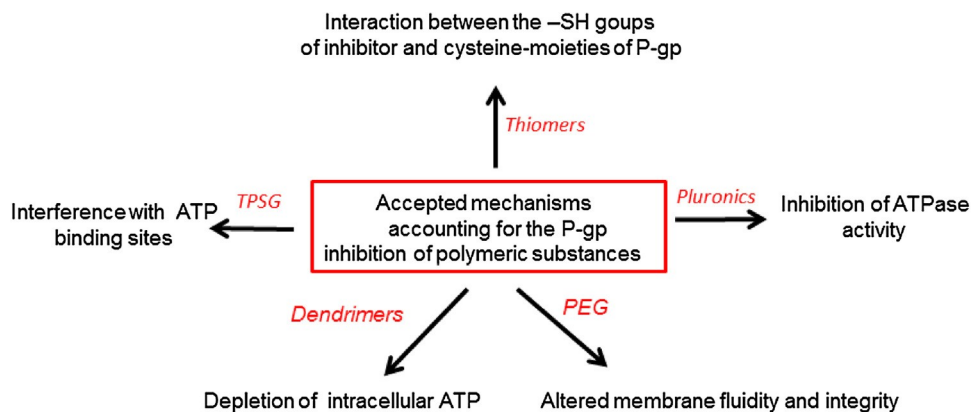


**Fig. 6.** Accepted mechanisms accounting for the P-gp inhibition of polymeric substances.

ity and depletion of intracellular ATP cannot be ruled out (Fig. 6) (Chen et al., 2015; Li et al., 2014).

## 5. Conclusions

Two main conclusions may be drawn from the results of the present work. First, the pre-treatment of efflux pump P-gp expressing Caco-2 cell monolayer with a GCS solution or GCS-based nanoparticles restores cell entrance of the P-gp substrate Rho-123

by blocking the efflux pump. Although essentially no difference occurs between the two dosage forms, it cannot be ruled out that, with P-gp substrates different from Rho-123, different behaviors may be observed between the dosage forms as for P-gp inhibition. Second, in sharp contrast to CS-TBA, the analogous conjugate GCS-TBA did not show any P-gp inhibitory activity and this thiomers cannot be useful for maximizing the P-gp inhibitory properties of GCS. It may be due to the decreased macromolecular flexibility of the latter conjugate which prevents an efficient interaction

with the Caco-2 cell membranes and change of their fluidity even though further mechanisms cannot be ruled out. Therefore, GCS and derived dosage forms may contribute to increase the oral bioavailability of Pgp-substrate drugs such as cyclosporine and paclitaxel with the notable advantage of using a commercially available polymer which does not require further chemical modification.

## 6. Declaration of interest

The authors declare no conflict of interest.

## Acknowledgments

This work was supported by grants from MIUR (Ministero dell'Istruzione, dell'Università e della Ricerca, Progetto PRIN 2011-2014 to A.T. and G.T.) and Università degli Studi di Bari (Progetti d'Ateneo to G.T.).

## References

- Benet, L. Z., Izumi, T., Zhang, Y., Silverman, J. A., & Wachter, V. J. (1999). Intestinal MDR transport proteins and P-450 enzymes as barriers to oral drug delivery. *Journal of Controlled Release*, *62*(1–2), 25–31.
- Bernkop-Schnürch, A., Hornof, M., & Zoidl, T. (2003). Thiolated polymersüthiomers: Synthesis and in vitro evaluation of chitosan–2-iminothiolane conjugates. *International Journal of Pharmaceutics*, *260*, 229–237.
- Bernkop-Schnürch, A. (2004). Thiomers: A new generation of mucoadhesive polymers. *Advanced Drug Delivery Reviews*, *57*, 1569–1582.
- Bonengel, S., & Bernkop-Schnürch, A. (2014). Thiomers — From bench to market. *Journal of Controlled Release*, *195*, 120–129.
- Britton, S., & Palacios, R. (1982). Systemic toxic effects associated with high-dose verapamil infusion and chemotherapy administration. *Immunological Reviews*, *65*, 5–22.
- Chan, L. M., Lowes, S., & Hirst, B. H. (2004). The ABCs of drug transport in intestine and liver: Efflux proteins limiting drug absorption and bioavailability. *European Journal of Pharmaceutical Sciences*, *21*(1), 25–51.
- Chen, X., Zhang, Y., Yuan, L., Zhang, H., Dai, W., He, B., Wang, X., & Zhang, Q. (2015). The P-glycoprotein inhibitory effect and related mechanisms of thiolated chitosan and its S-protected derivative. *RSC Advances*, *5*, 104228–104238.
- Colabufo, N. A., Berardi, F., Cantore, M., Perrone, M. G., Contino, M., Inglese, C., et al. (2008). Small P-gp modulating molecules: SAR studies on tetrahydroisoquinoline derivatives. *Bioorganic & Medicinal Chemistry*, *16*, 362–373.
- Colabufo, N. A., Berardi, F., Cantore, M., Contino, M., Inglese, C., Niso, M., et al. (2010). Perspectives of P-glycoprotein modulating agents in oncology and neurodegenerative diseases: Pharmaceutical, biological and diagnostic potentials. *Journal of Medicinal Chemistry*, *53*, 1883–1897.
- Colabufo, N. A., Berardi, F., Perrone, M. R., Capparelli, E., Cantore, M., Inglese, C., et al. (2010). Substrates, inhibitors and activators of P-glycoprotein: Candidates for radiolabeling and imaging perspectives. *Current Topics in Medicinal Chemistry*, *10*, 1703–1714.
- Cordon-Cardo, C., O'Brien, J. P., Boccia, J., Casals, D., Bertino, J. R., & Melamed, M. R. (1990). Expression of the multidrug resistance gene product (P-glycoprotein) in human normal and tumor tissues. *Journal of Histochemistry & Cytochemistry*, *38*, 1277–1287.
- Dünnhaupt, S., Barthelmes, J., Rahmat, D., Leithner, K., Thurner, C. C., Friedl, H., et al. (2012). S-protected thiolated chitosan for oral delivery of hydrophilic macromolecules: evaluation of permeation enhancing and efflux pump inhibitory properties. *Molecular Pharmaceutics*, *9*(5), 1331–1341.
- Di Gioia, S., Trapani, A., Mandracchia, D., De Giglio, E., Cometa, S., Mangini, V., et al. (2015). Intranasal delivery of dopamine to the striatum using glycol chitosan/sulfobutylether- $\beta$ -cyclodextrin based nanoparticles. *European Journal of Pharmaceutics and Biopharmaceutics*, *94*, 180–193.
- Dong, X., Mattingly, C. A., Tseng, M. T., Cho, M. J., Liu, Y., Adams, V. R., et al. (2009). Doxorubicin and paclitaxel-loaded lipid-based nanoparticles overcome multidrug resistance by inhibiting P-glycoprotein and depleting ATP. *Cancer Research*, *69*, 3918–3926.
- Foger, F., Schmitz, T., & Bernkop-Schnürch, A. (2006). In vivo evaluation of an oral delivery system for P-gp substrates based on thiolated chitosan. *Biomaterials*, *27*, 4250–4255.
- Gupta, P., Garg, T., Tanmay, M., & Arora, S. (2015). Polymeric drug-delivery systems: Role in P-gp efflux system inhibition. *Critical Reviews™ in Therapeutic Drug Carrier Systems*, *32*(3), 247–275.
- Hunter, J., & Hirst, B. H. (1997). Intestinal secretion of drugs. The role of P-glycoprotein and related drug efflux systems in limiting oral drug absorption. *Advanced Drug Delivery Reviews*, *25*, 129–157.
- Juliano, R. L., & Ling, V. (1976). A surface glycoprotein modulating drug permeability in Chinese hamster ovary cell mutants. *Biochimical Biophysical Acta*, *455*, 152–162.
- Lee, S. J., Huh, M. S., Lee, S. Y., Min, S., Lee, S., Koo, H., et al. (2012). Tumor-homing poly-siRNA/glycol chitosan self-cross-linked nanoparticles for systemic siRNA delivery in cancer treatment. *Angewandte Chemie International Edition*, *51*, 7203–7207.
- Leopoldo, M., Lacivita, E., De Giorgio, P., Colabufo, N. A., Niso, M., Berardi, F., et al. (2006). Design synthesis, and binding affinities of potential positron emission tomography (PET) ligands for visualization of brain dopamine D3 receptors. *Journal of Medicinal Chemistry*, *49*, 358–365.
- Li, Z., Cho, S., Kwon, I. C., Janát-Amsbury, M. M., & Huh, K. M. (2013). Preparation and characterization of glycol chitin as a new thermogelling polymer for biomedical applications. *Carbohydrate Polymers*, *92*, 2267–2275.
- Li, W., Li, X., Gao, Y., Zhou, Y., Ma, S., Zhao, Y., et al. (2014). Inhibition mechanism of P-glycoprotein mediated efflux by mPEG-PLA and influence of PLA chain length on P-glycoprotein inhibition activity. *Molecular Pharmaceutics*, *11*(January (1)), 71–80.
- Mandracchia, D., Denora, N., Franco, M., Pitarresi, G., Giammona, G., & Trapani, G. (2011). New biodegradable hydrogels based on inulin and  $\alpha$ ,  $\beta$ -polyaspartylhydrazide designed for colonic drug delivery: In vitro release of glutathione and oxytocin. *Journal of Biomaterials Science, Polymer Edition*, *22*(1–3), 313–328.
- Mattioli Belmonte, M., Cometa, S., Ferretti, C., Iatta, R., Trapani, A., Ceci, E., et al. (2014). Characterization and cytocompatibility of an antibiotic/chitosan/cyclodextrins nanocoating on titanium implants. *Carbohydrate Polymers*, *110*, 173–182.
- Mazzafarro, S., Bouchemal, K., & Ponchel, G. (2013a). Oral delivery of anticancer I: General considerations. *Drug Discovery Today*, *18*, 25–34.
- Mazzafarro, S., Bouchemal, K., & Ponchel, G. (2013b). Oral delivery of anticancer III: Formulation using drug delivery systems. *Drug Discovery Today*, *18*, 99–104.
- Muzzalupo, R., Iemma, F., Picci, N., Pitarresi, G., Cavallaro, G., & Giammona, G. (2001). Novel water-swellable beads based on an acryloylated polyaspartamid. *Colloid and Polymer Science*, 688–695.
- Pang, L., Qin, J., Han, L., Zhao, W., Liang, J., Xie, Z., et al. (2016). Exploiting macrophages as targeted carrier to guide nanoparticles into glioma. *Oncotarget*, *7*(24), 37081–37091. <http://dx.doi.org/10.18632/oncotarget.9464> [www.impactjournals.com/oncotarget](http://www.impactjournals.com/oncotarget)
- Pennock, G. D., Dalton, W. S., Roeske, W. R., Appleton, C. P., Mosley, K., Plezia, P., et al. (1991). Systemic toxic effects associated with high-dose verapamil infusion and chemotherapy administration. *Journal of the National Cancer Institute*, *83*, 105–110.
- Pitarresi, G., Pierno, P., Tripodo, G., Mandracchia, D., & Giammona, G. (2005). Drug delivery from mucoadhesive disks based on a photo-crosslinkable polyaspartamide derivatives. *Journal of Drug Delivery Science and Technology*, *15*, 377.
- Rossi, S., Ferrari, F., Bonferoni, M. C., & Caramella, C. (2000). Characterization of chitosan hydrochloride-mucin interaction by means of viscosimetric and turbidimetric measurements. *European Journal of Pharmaceutical Sciences*, *10*, 251–257.
- Tang, S. C., Lagas, J. S., Lankheet, N. A., Poller, B., Hillebrand, M. J., Rosing, H., et al. (2012). Brain accumulation of sunitinib is restricted by P-glycoprotein (ABCB1) and breast cancer resistance protein (ABCG2) and can be enhanced by oral elacridar and sunitinib coadministration? *International Journal of Cancer*, *130*(1), 223–233.
- Thermes, F., Grove, J., Rozier, A., Plazonnet, B., Constancis, A., Bunel, C., et al. (1992). Mucoadhesion of copolymers and mixtures containing polyacrylic acid. *Pharmaceutical Research*, *9*, 1563–1567.
- Thiebaut, F., Tsuruo, T., Hamada, H., Gottesman, M. M., Pastan, I., & Willingham, M. C. (1987). Cellular localization of the multidrug-resistance gene product P-glycoprotein in normal human tissues. *Proceedings of the National Academy of Sciences of the United States of America*, *84*, 7735–7738.
- Trapani, G., Franco, M., Trapani, A., Lopodota, A., Latrofa, A., Gallucci, E., et al. (2004). Frog intestinal sac: A new in vitro method for the assessment of intestinal permeability. *Journal of Pharmaceutical Sciences*, *93*(12), 2909–2919.
- Trapani, A., Palazzo, C., Contino, M., Perrone, M. G., Cioffi, N., Ditaranto, N., et al. (2014). Mucoadhesive properties and interaction with P-glycoprotein (P-gp) of thiolated-chitosans and  $\beta$ -glycol chitosans and corresponding parent polymers: A comparative study. *Biomacromolecules*, *15*, 882–893.
- Werle, M. (2008). Natural and synthetic polymers as inhibitors of drug efflux pump. *Pharmaceutical Research*, *25*, 500–511.
- Wong, H. L., Bendayan, R., Rauth, A. M., Xue, H. Y., Babakhanian, K., & Wu, X. Y. (2006). A mechanistic study of enhanced doxorubicin uptake and retention in multidrug resistant breast cancer cells using a polymer-lipid hybrid nanoparticle system. *Journal of Pharmacology and Experimental Therapeutics*, *317*, 1372–1381.
- Yhee, J. Y., Song, S., Lee, S. J., Park, S. G., Kim, K. S., Kim, M. G., et al. (2015). Cancer-targeted MDR-1 siRNA delivery using self-cross-linked glycol chitosan nanoparticles to overcome drug resistance. *Journal of Controlled Release*, *198*, 1–9.
- Zhao, B., Wang, X. Q., Wang, X. Y., Dai, W. B., Wang, J., Zhong, Z., et al. (2013). Nanotoxicity comparison of four amphiphilic polymeric micelles with similar hydrophilic or hydrophobic structure. *Particle and Fibre Toxicology*, *10*, 47. <http://dx.doi.org/10.1186/1743-8977-10-47>